Received: 14 October 2019 | Revised: 14 October 2019 | Accepted: 7 January 2020

DOI: 10.1111/ijac.13471

ORIGINAL ARTICLE

International Journal of Applied Ceramic TECHNOLOGY

The effect of Dy^{3+} doping on the thermoluminescence properties of Ba_2SiO_4

Vural E. Kafadar[1] | **Tuncay Yeşilkaynak**[2] | **Ruken Esra Demirdogen**[3] | **Awara A. Othman**[1] | **Fatih Mehmet Emen**[4] | **Selma Erat**[5,6]

[1]Department of Engineering Physics, University of Gaziantep, Gaziantep, Turkey

[2]Afsin Vocational School, Kahramanmaraş Sütcü İmam University, Kahramanmaraş, Turkey

[3]Department of Chemistry, Faculty of Science, Çankırı Karatekin University, Çankırı, Turkey

[4]Department of Chemistry, Faculty of Arts and Science, Mehmet Akif Ersoy University, Burdur, Turkey

[5]Advanced Technology, Research and Application Center, Mersin University, Mersin, Turkey

[6]Vocational School of Technical Sciences, Program of Opticianry, Department of Medical Services and Techniques, Mersin University, Mersin, Turkey

Correspondence
Vural E. Kafadar, University of Gaziantep, Department of Engineering Physics, Gaziantep, Turkey.
Email: kafadar@gantep.edu.tr

Funding information
Kahramanmaraş Sütçü İmam University Research Fund, Grant/Award Number: 2015/2-31M

Abstract

The thermoluminescence (TL) properties of barium silicate phosphor, Ba_2SiO_4:%3Dy^{3+} synthesized by using hydrothermal method were investigated and presented in detail. The crystallographic structure of Ba_2SiO_4:%3Dy^{3+} was determined by conventional x-ray diffraction technique and the results showed that the sample was grown in orthorhombic phase with *Pmcn* (62) space group (PDF: 01-077-0150). The excitation spectra of Ba_2SiO_4:Dy^{3+} were measured in the wavelength range of 220-400 nm and the spectra showed that there were several excitation bands in the sample. The CIE chromaticity coordinates were also calculated from emission spectra for Dy^{3+}-doped Ba_2SiO_4. In order to calculate the kinetic parameters of the sample the additive dose, peak shape and computerized glow curve deconvolution methods were used. It was found that Ba_2SiO_4:Dy^{3+} was composed of five general order TL glow peaks. The fading characteristics of the sample were also studied over a period time. At the end of the planned storage times, the normalized TL peak area of Ba_2SiO_4:Dy^{3+} reduced 60% of its original value.

KEYWORDS

Ba_2SiO_4:Dy^{3+}, kinetic parameters, photoluminescence, thermoluminescence

1 | INTRODUCTION

Thermoluminescence (TL) dosimeters are helpful in many radiation fields due to their favorable properties high sensitivity, small in size, possible point dose measurement, many existing in various forms, not expensive, reasonably equivalent tissue, and have found many useful applications in various fields, such as personnel and environmental monitoring, retrospective dosimetry, medical dosimetry, space dosimetry, and high-dose dosimetry.[1] Many researchers used barium silicate as the host material in thermoluminescence studies and they used different methods to achieve the various form of it. Yamaga et al in 2005 studied barium silicate (Ba_2SiO_4) and (Ba_3SiO_5) that was doped by Eu^{2+}, barium silicate radiated with UV light and the broadband luminescence of (Ba_2SiO_4) and (Ba_3SiO_5) produced with peak wavelengths of 510 and 590 nm, respectively. Yamaga et al reported that the produced electrons and holes by UV excitation in the crystal through thermal hopping and tunneling moved back to Eu^{2+} sites and at Eu^{2+} recombine radiatively.[2] Yao et al in 2010 studied the photoluminescence properties of $Ba_2ZnSi_2O_7$:Eu^{2+},Re^{3+} (Re = Dy, Nd) prepared by using the combustion-assisted synthesis (CAS) technique. A single band that centered at 503 nm was observed in the emission spectrum, which

corresponds to the $4f^6 5d^1 \rightarrow 4f^7$ transition of Eu^{2+} when the $Ba_2ZnSi_2O_7$:Eu phosphors doped by Dy^{3+} and Nd^{3+} ions, then the blue-green afterglow $\lambda_{em} = 503\,nm$ was observed.[3] Wang et al in 2010 studied bluish-green long-lasting phosphorescent phosphor of N contained Ba_2SiO_4:Eu^{2+} for x-ray and cathode-ray tubes. They reported that with increasing the content of Si_3N_4, the phosphorescence grows super-linearly and some new TL peaks appear at low temperatures of about 335, 355, 365, and 400 K. These peaks are attributed to the formation of new traps related to the N substitution for O.[4] Sakamoto et al in 2011 succeeded in the growth of single crystal of Ba_2SiO_4:Eu^{2+} by novel synthesis method which included SiO in gas phase and Ba–Sc–Al–Eu–O in solid phase hybridized. They were able to synthesize Ba_2SiO_4:Eu^{2+} single crystal by interfacial crystal growth after the reaction of the SiO gas with the surface of Ba–Sc–Al–Eu–O substrate in the reductive atmosphere. It was reported that single crystal has about 500 μm sizes and emits green light at around 500 nm under 300-450 nm excitation.[5] Huayna et al in 2013 studied the red, green, and blue photoluminescence of Ba_2SiO_4: M (M = Eu^{3+},Eu^{2+},Sr^{2+}). Energy and time-saving combustion synthesis were applied flexibly to the preparation of doped and un-doped barium orthosilicate nanoparticles (NPs) resulting in very small nanoparticles with a size of about 35 nm. Different approaches were used to obtain red-green-blue emission and Ba_2SiO_4 NPs was doped with Eu^{3+}, Eu^{2+}, and Sr^{2+}, respectively. Substitution of Ba^{2+} ions with Sr^{2+} ions leads to lattice defects, which are stabilized by in situ lattice imperfections of Ba_2SiO_4 nanocrystals.[6] Wang et al in 2015 reported the sunlight activated long-lasting luminescence from $Ba_5Si_8O_{21}$:Eu^{2+},Dy^{3+} phosphor. Persistent phosphors of visible light are commonly used as freestanding night vision and fluorescent labeling materials.[7] Zhang et al in 2017 studied the enhancement of the stability of green-emitting Ba_2SiO_4:Eu^{2+} phosphor by hydrophobic modification. A hydrophobic surface layer was formed on the surface of this phosphor by hydrolysis and polymerization of tetraethylorthosilicate (TEOS) and polydimethylsiloxane (PDMS). The surface layer produced consisted of an amorphous silicon dioxide with a thickness of ~2 nm with the presence of $–CH_3$ groups on the surface. The modified phosphorus exhibited superior stability under high-pressure water vapor conditions at 150°C.[8] Alkaline earth silicates have been studied by several researchers as useful luminescent hosts with a stable crystal structure and high physical and chemical stability. Different silicate hosts have various effects around activator ions.[9,10] Alkaline earth metal (Ca, Sr, Ba) silicate attracts a great deal of attention as there is a relatively wide band gap suitable for the sustained luminescent center of Eu^{2+} and Ce^{3+},[11,12] and it has several reports dealing with the luminescence properties of Sr_2SiO_4, $Ca_2MgSi_2O_7$, $Sr_2MgSi_2O_7$, $Sr_3MgSi_2O_8$, and $Ca_3MgSi_2O_8$ in literature.[13–15] However, few journalists treat Ba_2SiO_4 as TL material.

In the present paper, Ba_2SiO_4:Dy^{3+} was synthesized by hydrothermal technique in order to investigate the effect of Dy^{3+} doping on the thermoluminescence (TL) properties of Ba_2SiO_4. The conventional x-ray diffraction (XRD) technique was used to chracterize the crystalographic structure of Ba_2SiO_4:Dy^{3+}. The Additive Dose (AD), Peak Shape (PS), and Computerized Glow Deconvolution (CGCD) methods were used to determine the kinetic parameters namely the order of kinetics (b), activation energy (E_a), and the frequency factor (s) associated with the dosimetric thermoluminescence (TL) glow peaks of Ba_2SiO_4:Dy^{3+}.

2 | MATERIALS AND METHOD

Barium nitrate (99%), Dysprosium (III) oxide (99%), Polyethylene glycol 10 000 (100%), and Citric acid (99%) were purchased from Merck. As a solution solvent, ethanol (≥99.9%) was purchased from Merck. All the reagents were used as received without further purification. 3% Dy^{3+}-doped Barium silicate was synthesized by Hydrothermal Method. 2×10^{-3} mol Ba $(NO_3)_2$ in 15 mL of purified water, 1×10^{-3} mol SiO_2 xH_2O in pure water or TEOS (twice the molar ratio of polyethylene glycol with TEOS will be used) in 15 mL ethanol and 0.2 g citric acid in 10 mL pure water were dissolved separately. Dysprosium (III)nitrate hydrate was dissolved in 5 mL of purified water. The solutions of the metal salts mixed with the citric acid solution. Then Ba $(NO_3)_2$ solution was added and the mixture was stirred with a magnetic stirrer at room temperature for 10 minutes. The pH of the homogeneous solution adjusted to 12 with 5 mol/L NaOH and mixed before taking up the hydrothermal reactor. The pH adjustment was achieved by using a PH meter. The mixture was put into the Teflon reactor left for 1 hour and then it was taken to the hydrothermal unit. The temperature was set at 393-453 K and held at high pressure for 12-18 hours and the oven was turned off and slowly cooled down to room temperature (RT). After cooling the hydrothermal reactor to RT, the precipitate was separated by centrifugation and dried at 333 K for 12 hours. Ba_2SiO_4:Dy^{3+} was heated for 3 hours at the required temperature (1523-1623 K).

The structure of Ba_2SiO_4:Dy^{3+} was characterized by XRD in the range of diffraction angle $20° \leq 2\theta \leq 70°$ using a 0.021° step with 20 kV at 40 mA, Cu$K\alpha$ (1.54 Å) incident radiation. The morphological investigations of the phosphor were carried out via a LEO440 Computer Controlled Digital Scanning Electron Microscope. Photoluminescence (PL) measurements were made by using a Varian Cary Eclipse Fluorescence spectrophotometer. PL spectra were obtained at room temperature and excitation and emission slits were arranged as 20 and 10, respectively. The phosphor was irradiated at room temperature by a beta source from a calibrated emitter ^{90}Sr–^{90}Y. Strontium

−90 from their daughter products (^{90}Sr β- 8.73 × 10^{-14} J together with ^{90}Y β-3.63 × 10^{-13} J) emits high energy beta particles (0.04 Gy/s). Harshaw QS 3500 TLD reader system was used to read out the irradiated sample. This system is a manual type reader which is computer interfaced to hand operator, TLD reader system and program that run on WinREMS.

3 | RESULTS AND DISCUSSION

The crystallographic structure of Ba_2SiO_4:Dy^{3+} was characterized by using the conventional XRD technique. Figure 1 shows the x-ray diffractogram of the sample and also the comparison with the reference of Ba_2SiO_4 (PDF: 01-077-0150). It is easy to observe that the patterns of the sample are well coincided with the patterns of the reference. Thus, the structure is determined as orthorhombic crystal system with Pmcn (62) space group and unit cell parameters of $a = 5.8050$ Å, $b = 10.200$ Å, $c = 7.4990$ Å; $\alpha = \beta = \gamma = 90°$. It is difficult to observe any significant changes in the structure due to doping 3% Dy^{3+} into Ba_2SiO_4. The ionic radius of Dy^{3+} (1.027 Å) is close to that of Ba^{2+} (1.42 Å) in the eightfold coordination. The ionic radius of Si^{4+}, which is 0.26 Å in the fourfold coordination, is too small to host Dy^{3+}. Therefore, the Ba^{2+} ions are replaced by Dy^{3+} instead of Si^{4+} ions. According to these results, the formula of the phosphor can be given as $Ba_{1.97}Dy_{0.03}SiO_4$.

The surface morphology of Ba_2SiO_4:Dy^{3+} investigated by SEM image analysis is given in Figure 2. SEM micrographs with 10000× magnification indicate that average grain size in the obtained (Ba_2SiO_4:Dy^{3+}) phosphor is in the range of 230-650 nm. The micro-structures of the phosphors consisted of regular fine grains and crystalline structures with sharp boundaries.

The excitation and emission spectrums of the Ba_2SiO_4:Dy^{3+} are presented in Figure 3. The excitation spectrum can be investigated in two parts. The first part, which is in between 200 and 320 nm, is the intense peak centered at 290 nm. The intense band is observed due to overlap of the charge transfer (CT) transitions of the host lattice from O^{2-}→Si^{4+} while the latter arises from the activator O^{2-}→Dy^{3+} groups. The other part of the excitation spectrum shows weak excitation bands in the range of 325-400 nm corresponding to electron transitions of Dy^{3+} ions from 6H15/2 → 4M17/2 (325 nm),[16] 6H15/2→4M15/2 (365 nm),[17] 6H15/2→6P7/2 (448 nm),[17,18] and 6H15/2→4I11/2 (351 nm).[17] The intense emission bands observed at 490 and 590 nm in the radiation spectrum belong to the 4F9/2→6H15/2 (490 nm)[19] and 4F9/2→6H13/2 (571 nm)[19] transitions of Dy^{3+} ions. Furthermore, low-intensity emission bands observed

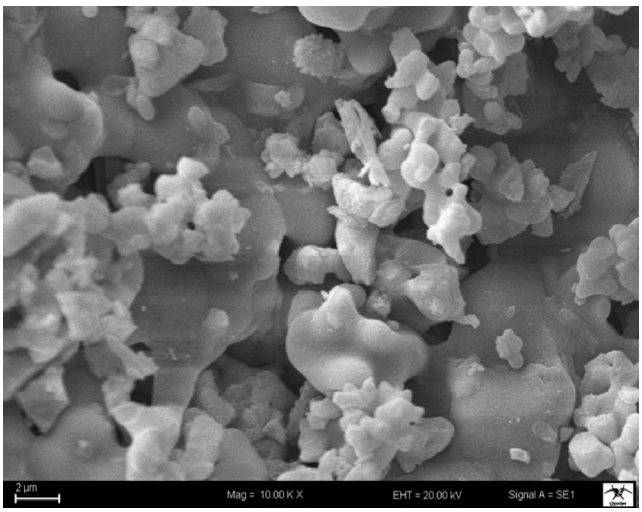

FIGURE 2 SEM micrograph of the Ba_2SiO_4:Dy^{3+} phosphor

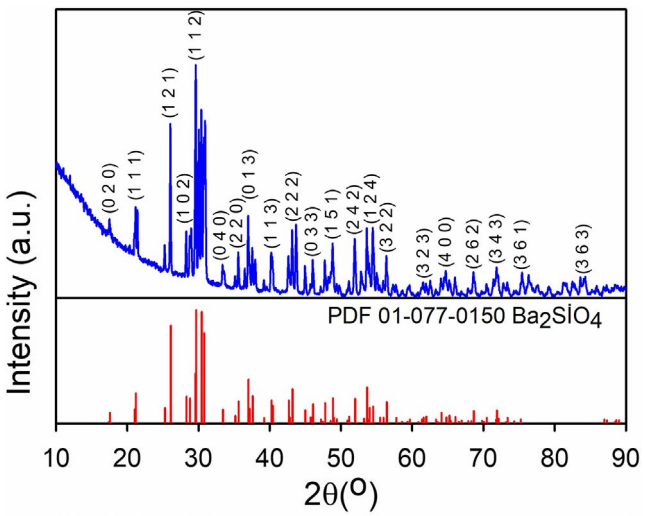

FIGURE 1 XRD patterns of the Ba_2SiO_4:Dy^{3+} phosphor

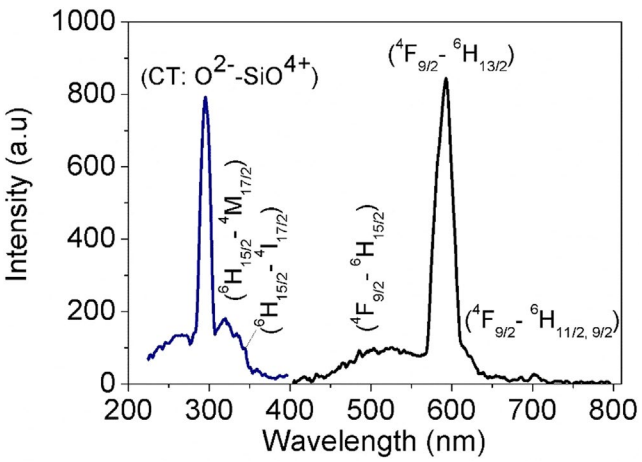

FIGURE 3 Excitation end emission spectrum of barium silicate (Ba_2SiO_4:Dy^{3+})

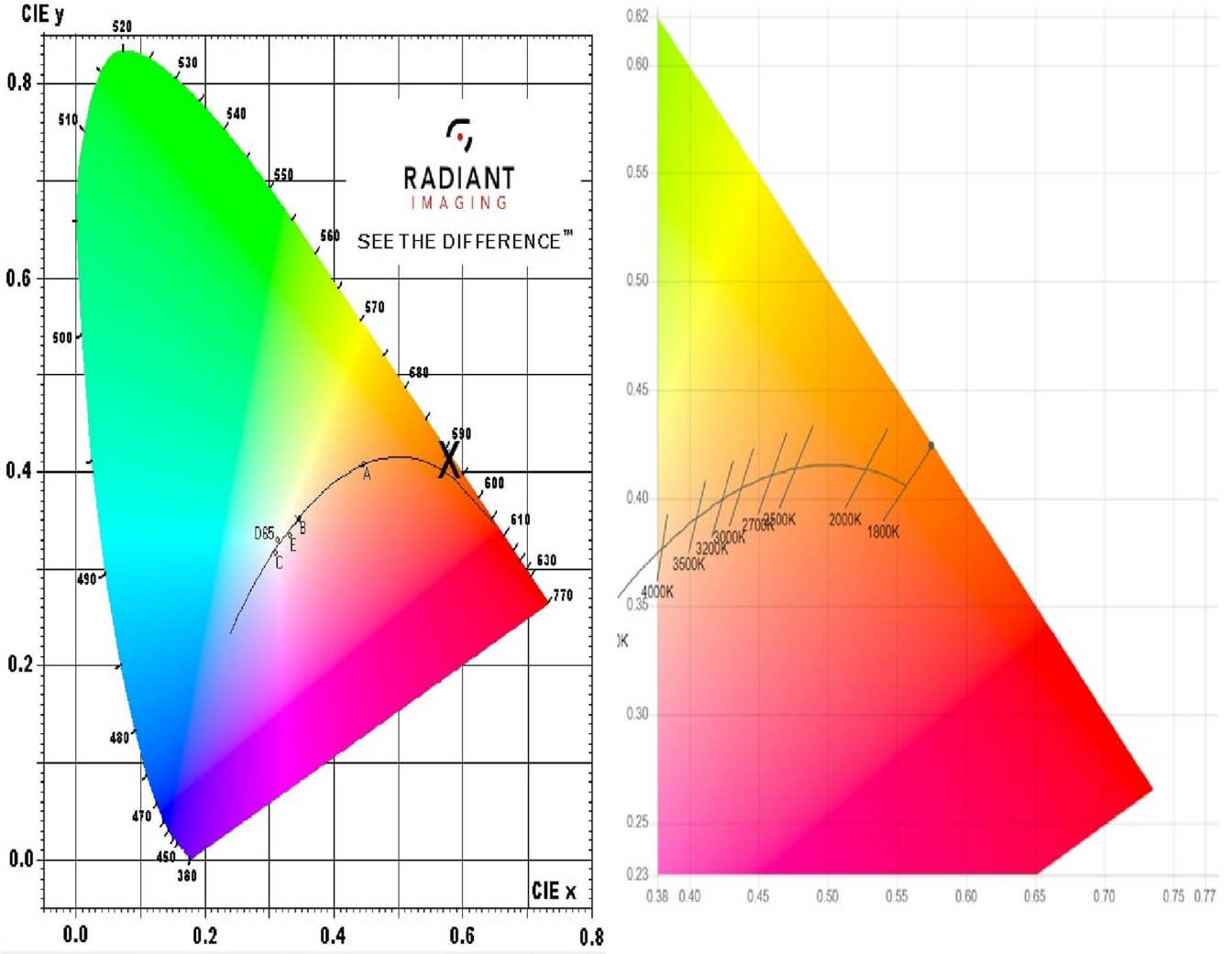

FIGURE 4 The graphs of CIE coordinates and color temperature

between 650 and 800 nm belong to the transition of $^4F_{9/2} \rightarrow {}^6H_j$ ($j = 11/2, 9/2$) of Dy^{3+} ions.[17]

The Commission Internationale deI'Eclairage (CIE) chromaticity coordinates and color temperature of Dy^{3+}-doped Ba_2SiO_4 was calculated from emission spectrum. CIE and Color temperature graphs are given in Figure 4. The location of color coordinates is represented in CIE chromaticity diagram by x. It was determined the color of Dy^{3+}-doped Ba_2SiO_4 is located in green-orange region. Color coordinates were calculated from the emission spectrum for the emission peak of 490 nm as $X = 0.575151311$ and $y = 0.424232235$. The color temperature was calculated to be 1800 K.

The dose-response behavior of the (Ba_2SiO_4:Dy^{+3}) was also investigated. The experiment conducted to investigate the effect of dose dependence at a peak position, and for this aim the samples were irradiated by β-ray source between ≈0.08 Gy and ≈1.15 kGy. In each experiment 15 mg of the sample (that was in powder form) irradiated at room temperature and immediately readout. Figures 5 and 6 show some of the selected glow curve structures of Ba_2SiO_4: Dy^{+3} after different dose levels. In general, experimental tests showed that there was no major shift in the site of peak temperature and there is a slight change in temperature with increasing dose level. That is, the glow peak temperature gradually shifted to the higher temperature side as the dose level increased. Every peak reaches a maximum intensity at around (373 to 423 K) at different dose levels. There are several experimental techniques such as (Initial Rise (IR), Variable Heating Rate (VHR) and Peak Shape (PS)) methods for a single glow curve to evaluate the trapping parameters. In this study, the peak shape and CGCD methods have been applied for evaluating trapping parameter of the main dosimeter peak of Dy^{+3}-doped Ba_2SiO_4. Previous studies have shown that the evaluation of the activation energy and the frequency coefficient depends mainly on knowledge of the kinetic order (b) and that the glow peak depends on the correct number of glow curves.[20] Another important subject in the application of geological dating, archeological, environmental, and personal dosimeters, and also in dosimeters studies is the

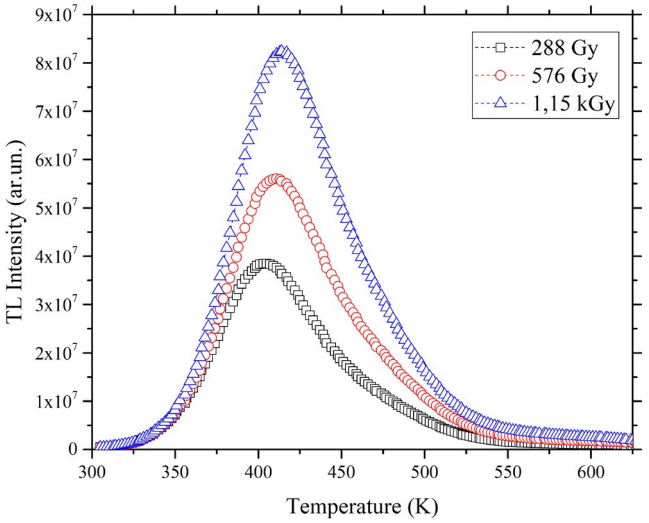

FIGURE 5 Typical glow curves of $Ba_2SiO_4:Dy^{3+}$ exposed to β rays ($\beta = 1$ K/s)

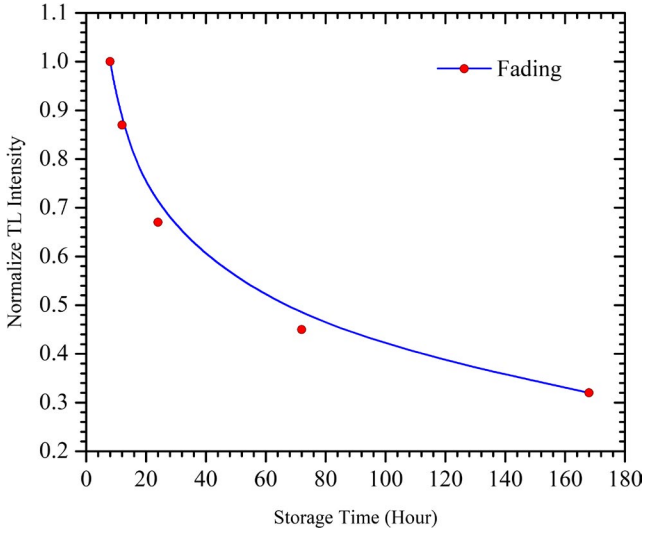

FIGURE 7 Normalized TL intensity for $Ba_2SiO_4:Dy^{3+}$ after various storage times at RT with 36 Gy and $\beta = 1$ K/s)

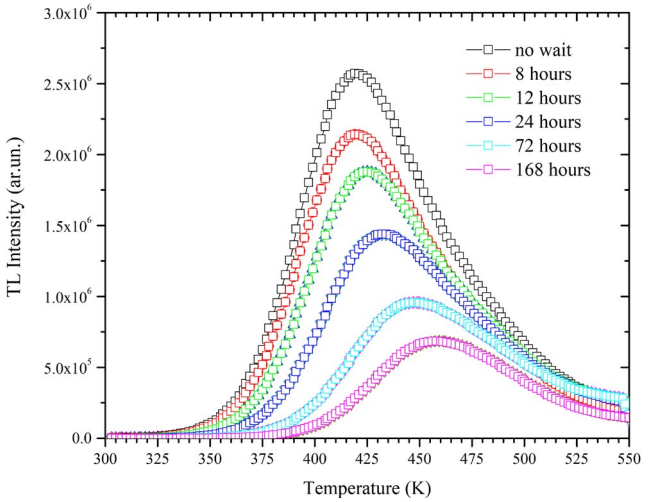

FIGURE 6 A set of TL glow curves for $Ba_2SiO_4:Dy^{3+}$ after various storage periods at RT. ($D = 36$ Gy, $\beta = 1$ K/s)

stability of signals stored at room temperature. The TL signal stored at room temperature decreases markedly during storage, will result from incompatibility in the result of emitted light and the exposure dose. A time-dependent decrease or loss of radiation-induced signals in a sample can lead to fading. Fading is a process that is an unintended loss of potential information that response occurs. The fading process has many causes, but thermal energy is the main thing. In thermal fading, as it is clear due to the high probability transition the fade faster for the trap that represents lower capture energy than the higher energy, due to this reason in dose evaluation large errors may generating.

In this experiment 15 mg of the sample ($Ba_2SiO_4:Dy^{3+}$) was used. The samples were irradiated 36 Gy and to avoid the effect of thermal fading and another external effect the sample is kept at room temperature in a dry and dark environment after irradiation for different time periods as shown in Figure 6. Moreover, Figure 6 also shows that maximum peak was located at temperature 418 K and shifted toward 458 K after 168 hours due to the shallow traps. This behavior is due to a decrease in the trapped charge concentration.[21] The change in the peak position is due to the presence of closely spaced trapping levels which progressively appear as the previous one fades.[22]

This result shows that the depth of the trap is dynamic during the decay process. In addition, this shifting in T_m indicates that the $Ba_2SiO_4:Dy^{3+}$ trapping system is more complex following the first-order kinetics from the Gaussian trap distribution. Additionally, it reiterates that the re-trapping influence cannot be ignored in the late stage of decay. Lastly, it can be seen that from the Figure 7, at the end of the planned storage times the normalized TL area of $Ba_2SiO_4:Dy^{3+}$ reduced 65% of its original value. The computerized glow curve deconvolution (CGCD) method has become a very popular way to obtain the kinetic parameters from the glow curves of TL materials. Therefore, the kinetic parameters such as number of glow peaks, activation energies (E_a), and kinetic order (b) for the dosimetric peaks of Dy^{3+}-doped Ba_2SiO_4 were obtained by CGCD method.[23] In this study, after many tries with different number of glow peaks, it was observed that the glow curve structures of $Ba_2SiO_4:Dy^{3+}$ is well described by a linear combination of at least five glow peaks. In this case, a reasonably good fit was always obtained. The obtained results of E_a, s, and b by using the CGCD methods are shown in Table 1.

$$I(T) = I_m \cdot b^{b/b-1} \cdot \exp\left(\frac{E}{kT} \cdot \frac{T - T_m}{T_m}\right) \times \left[(b-1)\cdot(1-\Delta)\cdot\frac{T^2}{T_m^2}\cdot\exp\left(\frac{E}{kT}\cdot\frac{T-T_m}{T_m}\right) + Z_m\right]^{-b/b-1}$$

TABLE 1 The trapping parameter values of the main dosimeter peak (P2) of $Ba_2SiO_4:Dy^{3+}$

	Chen PS			Mazumdar PS			
	E_τ	E_δ	E_ω	½ ratio	2/3 ratio	4/5 ratio	CGCD For P2
E_a (eV)	0.47	0.52	0.50	0.47	0.46	0.46	0.55
B	2	2	2	2	1.90	1.85	2
lns (s^{-1})	14.9	14.9	14.9	13.91	13.91	13.91	14.55

where;

$$\Delta = \frac{2kT}{E}, \Delta_m = \frac{2kT_m}{E}, Z_m = 1 + (b-1)\cdot\Delta_m$$

4 | CONCLUSION

$Ba_2SiO_4:Dy^{3+}$ was prepared by hydrothermal synthesis method and the thermoluminescence (TL) properties were investigated in detail. The foremost goal of our study was to find thermoluminescence kinetic parameters of Ba_2SiO_4 doped with Dy^{3+} after $^{90}Sr–^{90}Y$ β irradiation. These kinetic parameters are the order of kinetics (b), activation energy (E_a), and the frequency factor (s). These parameters are very helpful to understand the thermoluminescence properties of $Ba_2SiO_4:Dy^{3+}$. In this study, we used the Additive Dose experiment (AD) to examine the dose-dependent characteristics of the glow curve of barium silicate ($Ba_2SiO_4:Dy^{3+}$). Dose dependence was investigated by irradiating the sample at different dosage levels between ≈0.08Gy and ≈432Gy in the temperature range from RT to 673 K at a linear heating rate of 1 K/s. Experimental tests showed that there was no major shift in the site of peak temperature and there was a slight change in temperature and nearly constant with increasing dose levels. The value of kinetic parameters was founded by methods of Peak Shape (PS) and Computerized Glow Curve Deconvolution (CGCD) methods. In the storage time experiments the sample was irradiated by 36Gy and was kept for a different storage time period. At the end of the planned storage times the normalized TL area of $Ba_2SiO_4:Dy^{3+}$ reduced 65% of its original value. To solve this problem, we recommend adding multiple co-dopants to the host lattice. Therefore, our measurements provide some additional information on the properties of $Ba_2SiO_4:Dy^{3+}$.

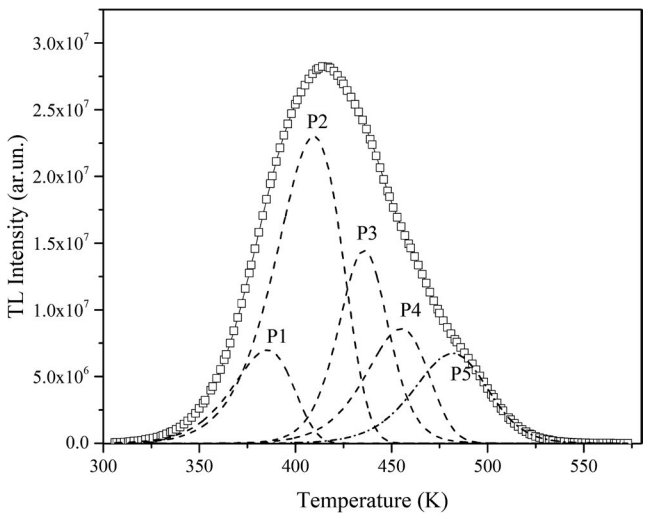

FIGURE 8 Computerized glow curve deconvolution results for $Ba_2SiO_4:Dy^{3+}$ measured after 144 Gy irradiation by β rays at RT with $\beta = 1$ K/s (FOM: 1.6)

ACKNOWLEDGMENTS

This work was supported by Kahramanmaraş Sütçü İmam University Research Fund (BAP-Project No. 2015/2-31M)

ORCID

Vural E. Kafadar https://orcid.org/0000-0002-0806-0943

REFERENCES

1. Bhatt BC, Kulkarni MS. Thermoluminescent phosphors for radiation dosimetry. Diffus Defect Data, Pt A. 2013;347:179–227.
2. Yamaga M, Masui Y, Sakuta S, Kodama N, Kaminaga K. Radiative and nonradiative decay processes responsible for long-lasting phosphorescence of Eu^{2+}-doped barium silicates. Phys Rev. 2005;71:205102.
3. Yao S, Li Y, Xue L, Yan Y. Photoluminescence properties of $Ba_2ZnSi_2O_7$: Eu^{2+}, Re^{3+} (Re= Dy, Nd) long-lasting phosphors prepared by the combustion-assisted synthesis method. J Alloys Compd. 2010;490:200–3.
4. Wang M, Zhang X, Hao Z, Ren X, Luo Y, Wang X, et al. Enhanced phosphorescence in N contained Ba_2SiO_4: Eu^{2+} for x-ray and cathode-ray tubes. Opt Mater. 2010;32:1042–5.
5. Sakamoto T, Uematsu K, Ishigaki T, Toda K, Sato M. Development of gas-solid phase hybrid synthesis method of single crystal Ba_2SiO_4: Eu^{2+}. Key Eng Mater. 2011;485:325–8.
6. Streit HC, Kramer J, Suta M, Wickleder C. Red, green, and blue photoluminescence of Ba_2SiO_4: M (M= Eu^{3+}, Eu^{2+}, Sr^{2+}) nano-phosphors. MDPI. 2013;6:3079–93.
7. Wang P, Xu X, Zhou D, Yu X, Qiu J. Sunlight activated long-lasting luminescence from $Ba_5Si_8O_{21}$: Eu^{2+}, Dy^{3+} phosphor. Inorg Chem. 2015;54:1690–7.
8. Zhang B, Zhang JW, Zhong H, Hao LY, Xu X, Agathopoulos S, et al. Enhancement of the stability of green-emitting Ba_2SiO_4: Eu^{2+} phosphor by hydrophobic modification. Mater Res. 2017;92:46–51.
9. Yamazaki K, Nakabayashi H, Kotera Y, Ueno A. Fluorescence of Eu^{2+}-activated binary alkaline earth silicate. J Electrochem Soc. 1986;133:657–60.
10. Barry TL. Equilibria and Eu^{2+} luminescence of subsolidus phases bounded by $Ba_3MgSi_2O_8$, $Sr_3MgSi_2O_8$, and $Ca_3MgSi_2O_8$. J Electrochem Soc. 1968;115:733–8.

11. Dorenbos P. Mechanism of persistent luminescence in $Sr_2MgSi_2O_7$: Eu^{2+}; Dy^{3+}. Phys Status Solidi B Basic Res. 2005;242:R7–R9.
12. Clabau F, Rocquefelte X, Jobic S, Deniard P, Whangbo MH, Garcia A, et al. Mechanism of phosphorescence appropriate for the long-lasting phosphors Eu^{2+}-doped $SrAl_2O_4$ with co-dopants Dy^{3+} and B^{3+}. Chem Mater. 2005;17:3904–12.
13. Lee JH, Kim YJ. Photoluminescent properties of Sr_2SiO_4: Eu^{2+} phosphors prepared by solid-state reaction method. Mat Sci Eng B-Adv. 2008;146:99–102.
14. Poort SHM, Reijnhoudt HM, Van der Kuip HOT, Blasse G. Luminescence of Eu^{2+} in silicate host lattices with alkaline earth ions in a row. J Alloys Compd. 1996;241:75–81.
15. Barry TL. Fluorescence of Eu^{2+}-activated phases in binary alkaline-earth orthosilicate systems. J Electrochem Soc. 1968;115:1181–4.
16. Zhang ZW, Song AJ, Ma MZ, Zhang XY, Yue Y, Liu RP. A novel white emission in $Ca_8MgBi(PO_4)_7$: Dy^{3+} single-phase full-color phosphor. J Alloys Compd. 2014;601:231–3.
17. Zhu G, Wang Y, Wang Q, Ding X, Geng W, Shi Y. A novel white emitting phosphor of Dy^{3+} doped $Ca_{19}Mg_2(PO_4)_{14}$ for light-emitting diodes. J Lumin. 2014;154:26–250.
18. Zhang Z, Song A, Shen X, Lian Q, Zheng X. A novel white emission in $Ba_{10}F_2(PO_4)_6$:Dy^{3+} single-phase full-color phosphor. Mater Chem Phys. 2015;151:345–50.
19. Liu F, Liu Q, Fang Y, Zheng N, Yang B, Zhao G. White light emission from $NaLa(PO_3)_4$:Dy^{3+} single-phase phosphors for light-emitting diodes. Ceram Int. 2015;41:1917–20.
20. Kitis G, Pagonis V. Peak shape methods for general order thermoluminescence glow-peaks: a reappraisal. Nucl Instrum Methods Phys Res. 2007;262:313–22.
21. Chen R, McKeever SWS. Theory of thermoluminescence and related phenomena. Singapore: World Scientific Publishing Co Pte. Ltd., 1997.
22. Thomas S, Kalita JM, Chithambo ML, Ntwaeaborwa OM. The influence of dopants on thermoluminescence of $Sr_2MgSi_2O_7$. J. Lumin. 2019;208:104–7.
23. Afouxenidis D, Polymeris GS, Tsirliganis NC, Kitis G. Computerised curve deconvolution of TL/OSL curves using a popular spreadsheet program. Radiat Prot Dosim. 2012;149:363–70.

How to cite this article: Kafadar VE, Yeşilkaynak T, Demirdogen RE, Othman AA, Emen FM, Erat S. The effect of Dy^{3+} doping on the thermoluminescence properties of Ba_2SiO_4. *Int J Appl Ceram Technol*. 2020;00:1–7. https://doi.org/10.1111/ijac.13471